大韓獸醫學會誌(2007) 第47卷 第2號
Korean J Vet Res(2007) 47(2) : 247~254

CT characteristics of normal canine pulmonary arteries and evaluation of optimal contrast delivery methods in CT pulmonary angiography

Joohyun Jung, Jinhwa Chang, Junghee Yoon, Mincheol Choi*

College of Veterinary Medicine, Seoul National University, Seoul 151-742, Korea
(Accepted: April 6, 2007)

Abstract : This study was performed to identify the normal anatomic orientation of pulmonary arteries and to obtain the normal baseline parameters and the optimal contrast material delivery methods of computed tomographic pulmonary angiography (CTPA) on normal beagle dogs. Based on the contrast injection flow rate, the contrast volume, and the administration methods, the experimental groups were divided into 4 groups such as group 1 : 2 ml/s, 3 ml/kg, and monophasic administration; group 2 : 5 ml/s, 3 ml/kg, and monophasic administration; group 3 : 5 ml/s, 4 ml/kg, and monophasic administration; group 4 : 5 ml/s and 2 ml/kg in first phase, 0.3 ml/s and 2 ml/kg in second phase, as biphasic administration. Normal anatomic orientation of pulmonary arteries in CTPA was evaluated through reformatted and 3D images after retro-reconstruction. Normal parameters for great arteries and peripheral pulmonary arteries were obtained on the factor of basement hounsfield unit (HU) values, contrast enhanced HU values, delay time, and peak time. And the optimal contrast delivery methods were evaluated on the factor of contrast enhanced HU values, image quality, and artifact. The monophasic administration with 5 ml/s contrast injection flow rate and 3 ml/kg contrast volume was optimal in canine CTPA.

Key words : anatomic orientation of pulmolnary arteries, computed tomographic pulmonary angiography (CTPA), dogs, normal parameters, optimal contrast delivery methods

Introduction

Pulmonary embolism (PE) occurs as a complication to a number of commonly encountered clinical diseases in veterinary medicine. The most common and representative underlying disease of PE in dogs was heartworm disease [3, 8, 17]. In addition, PE was identified in the case reports including cardiac disease, neoplasia, hyperadrenocorticism, disseminated intravascular coagulation, immune-mediated hemolytic anemia, systemic bacterial disease, sepsis [10, 13], cemented total hip arthroplasty [24], canine total hip replacement [14], *Blastomyces dermatitidis* [15], gross PE in a greyhound [1], medullary canal pressurization [16], renal amyloidosis [26], and nephrotic syndrome [19]. Through the retrospective study in dogs with confirmed PE, a variety of clinicopathologic and thoracic radiographic abnormalities were noted, however, there were no pathognomonic findings for PE [10, 13].

Computed tomography pulmonary angiography (CTPA) was first proposed as a diagnostic tool to evaluate pulmonary arterial diseases, including suspected PE in the 1980's [5, 12] in human medicine. CTPA is a computerized analysis for 2 dimensional images obtained from several different angles and 3 dimensional pictures after simple injection of contrast material through peripheral vein by using a small catheter to visualize blood flow in pulmonary arterial and venous vessels. Because of recent development of fast scanning techniques and routine use of contrast material injectors, CTPA has been a more noninvasive and comfortable method than pulmonary angiography and more specific than lung scintigraphy to approach to acute PE [18, 22, 23] and to manage chronic thromboembolic pulmonary hypertension [21] in human medicine. In addition, CTPA has the advantages of imaging the entire thorax and ruling out other diseases such as pneumonia and pulmonary neoplasia.

*Corresponding author: Mincheol Choi
College of Veterinary Medicine, Seoul National University, Seoul 151-742, Korea
[Tel: +82-2-880-1278, Fax: +82-2-880-8662, E-mail: mcchoi@snu.ac.kr]

However, optimal methods of CTPA and diagnostic analysis in canine pulmonary vasculatures were not well investigated. The purpose of this study was to determine the optimal contrast delivery methods of CTPA for diagnosis of pulmonary arterial diseases including PE, to acquire normal parameters of CTPA and to establish normal anatomic orientation of canine pulmonary arteries.

Materials and Methods

Helical CT examination

CT images were acquired using a single channel helical CT scanner, (GE CT/e; General Electric Medical System, Japan). In-plane pixel dimension was 512 × 512 pixels for all scans. The field of view ranged between 160 and 210 mm, using the smallest field of view. CT programs were used as follows; Cine scan (single level dynamic scan); retrospective reconstruction program; reformatted program (axial, sagittal, transverse, oblique plane); cross section histogram for measurement of Hounsfield unit (HU) values in 2D plane. A 22 G indwelling catheter placed in a cephalic vein of dogs was connected to CT power injector (LF CT9000 ADV; Liebel-Flarsheim, USA) through the control pressure line. Non-ionic iodine contrast media (Iohexol; Omnipaque 300 mgI; Amersham Health, Ireland) was used as the bolus injection technique by an automatic power injector. Dogs were anesthetized by isoflurane (Rhodia isoflurane soln; Hana Pharm, Korea) and hyperventilated prior to each scan to produce a period of apnea and avoid motion artifact. Cine scans at three regions, which included main pulmonary artery (MPA) region, bilateral second order arteries of MPA, and peripheral caudal segmental pulmonary arteries, were achieved under the conditions of 1 mm thickness, 120 kVp, 60 mA, 50 serial axial images and 1.5 second per 1 rotation. Delay time for CT angiography was obtained through time-attenuation curves achieved by using the hardwired basic CT program. Unenhanced and enhanced CT scan were acquired from thoracic inlet to diaphragm under conditions of 2 mm slice thickness, 2 mm interval, 1.3 pitch, 120 kVp, and 60 mA. All enhanced scan images were reconstructed to 0.5 mm multiplanar retro-reconstructed images and 3D images.

Experimental groups

Eight healthy beagle dogs, weighing 8~11.5 kg and ranging in 1~4 years were used without gender discrimination. Based on the contrast injection flow rate, contrast volume, and the administration methods, experimental groups were divided into 4 groups such as group 1: 2 ml/s, 3 ml/kg, and monophasic administration; group 2 : 5 ml/s, 3 ml/kg, and monophasic administration; group 3 : 5 ml/s, 4 ml/kg, and monophasic administration, group 4 : 5 ml/s and 2 ml/kg in first phase, 0.3 ml/s and 2 ml/kg in second phase as biphasic administration (Table 1).

Image analysis: HU values

Normal unenhanced basement hounsfield (HU) values and enhanced HU values of the MPA, right side MPA (R-MPA), left side MPA (L-MPA), right cranial lobar arteries (R-Cra), left cranial lobar arteries (L-Cra), right caudal lobar arteries (R-Cda), left caudal lobar arteries (L-Cda), accessory lobar arteries (ACa), aorta (AO), caudal vena cava (CVC), and lung parenchyma are acquired 3 times per dog in unenhanced and enhanced scan images. Regions of interest (ROI) were drawn in circular or ellipse up to a larger percentage (above about 70~80%) of vascular lumen but not escaped vessel outline using variable window setting. In lung parenchyma, ROI deposited carefully with avoiding small vessels using multiplanar reformatted images. The mean HU per voxel and the standard deviations of all HU values were recorded.

Image analysis: Time-attenuation curves

Time-attenuation data were used to find delay time of CTPA image acquisition following introvenous injection of contrast medium to maximize pulmonary arterial

Table 1. Experimental groups for the contrast delivery method

Groups	Contrast injection methods		
	Flow rate (ml/s)	Volume (ml/kg)	Administration
G1	2	3	Monophasic
G2	5	3	Monophasic
G3	5	4	Monophasic
G4	5	2	Biphasic (first)
	0.3	2	Biphasic (second)

opacification. On dynamic CT image, ROI was placed over the MPA, R-MPA, L-MPA, peripheral pulmonary arteries, AO, CVC, and within that region, HU value change according to time course was expressed as time-attenuation curve. Time was plotted on the x-axis in milliseconds, and the attenuation on the y-axis in HU value. To compensate for individual variations in circulation time, start of aortic enhancement (the point at which aortic attenuation began to rise above the baseline) was set to "zero time" in each set of data [6]. Each delay time was applied to enhanced scan time, respectively. Parameters for peak time, contrast enhanced HU values in peak time, delay time, initial enhanced time in delay time were acquired in all dogs.

Image analysis: Image quality and artifacts

A subjective CTPA image quality and artifacts evaluation with a 5 point score system using 2D reformatted images on monitor was performed by 3 veterinary radiologists according to the following described method. First, as CTPA image quality, the degree of arterial distension, mural visualization and arterial bifurcation visualization on CT images were graded using from 1 to 3 with half points; 1, none; 1.5, poor; 2, partial; 2.5, good; and 3, full distension and mural visualization. Second, as CTPA artifacts, false-positive PE-like regions were graded using a three-point scale from 1 to 3; 1, several false-positive; 2, small false-positive; 3, almost absence of false-positive result. All groups with total grades were compared.

Image analysis: Normal anatomic orientation of pulmonary arteries

Normal anatomic orientation of pulmonary arteries in CTPA was evaluated through the reformatted images and 3D images after 0.5 mm retro-reconstruction using various window settings. 3D SSD reconstruction was applied to threshold-based reconstruction technique. Threshold-based reconstruction is techniques that background of lower HU value was eliminated, the image more than set point (3D threshold) was remained.

Data analysis

Statistical analysis was performed using the SPSS (SPSS for Windows Release 13.0.0; SPSS, USA) statistical computer program. A one-way ANOVA least significant difference (LSD) test was applied to analyze data of enhanced HU values. For rating images on the basis of the image quality and artifacts for comparison with groups, Kruskal Wallis Test and Mann-Whitney U test were applied. Through Kruskal Wallis Test, all groups were compared as significant test. And Mann-Whitney U test was applied to compare each group.

Results

Basement HU values

Normal basement HU values for MPA, R-MPA, L-MPA, R-Cra, L-Cra, R-Cda, L-Cda, ACa, AO, CVC, and lung parenchyma were listed in Table 2. The HU value of R-MPA was higher than that of the L-MPA. The HU value of CVC around the heart was higher than that of CVC around the liver. However, there were no significant differences.

Delay time and peak time

MPA had a rapid rise at 3.25 second in attenuation and reached the peak HU value at 6.5 second at 5 ml/s contrast injection flow rate. AO had a rapid rise at 6.8 second in attenuation and reached the peak HU

Table 2. Basement HU values of canine pulmonary arteries (mean ± SD) (n = 32)

	HU value		HU value
MPA	28.33 ± 6.65	ACa	32.83 ± 8.58
R-MPA	38.83 ± 7.27	L-Cda	29.61 ± 8.07
L-MPA	31.72 ± 6.50	AO	32.61 ± 7.46
R-Cra	30.60 ± 10.45	CVC (H)	56.55 ± 9.30
L-Cra	29.05 ± 6.72	CVC (L)	30.67 ± 3.72
R-Cda	30.44 ± 6.59	Lung	−735.44 ± 119.56

MPA, main pulmonary artery; R-MPA, right side of main pulmonary artery; L-MPA, left side of main pulmonary artery; R-Cra, right cranial lobar artery; L-Cra, left cranial lobar artery; R-Cda, right caudal lobar artery; ACa, accessory lobar artery; L-Cda, left caudal lobar artery; AO, aorta; CVC (H), caudal vena cava in the level of heart; CVC (L), caudal vena cava in the level of liver.

value at 11.69 second. One interesting finding was that the delay time and peak time were slightly faster in R-Cda than in ACa and L-Cda. However, there were no significant differences between R-Cda, ACa, and L-Cda (Table 3).

Enhanced HU values

The Enhanced HU values of group 1 were lower than other groups in all regions ($p < 0.05$). The highest HU values in the region of MPA, peripheral arteries, AO, CVC were shown in the group 3 among all groups. In the region of MPA and AO, group 3 had the statistically significant higher HU values than other groups ($p < 0.05$). In the region of peripheral pulmonary arteries and CVC, there were no statistically significant differences among group 2, 3, and 4. The highest HU values in the region of R-MPA and L-MPA were in the group 4. However, there were no statistically significant differences among groups 2, 3, and 4 (Table 4).

Image quality and artifacts

In the factor of the image quality and loss of artifacts, group 1 was lower than other groups ($p < 0.05$). The best image quality and loss of artifacts were shown in the group 3. However, there were no statistically significant differences among groups 2, 3, and 4 (Fig. 1).

Normal anatomic orientations of canine pulmonary arteries

Pulmonary arteries of each lung lobes were confirmed anatomical locations and orientations through reformatted images and 3D reconstruction after 0.5 mm retroreconstruction (Fig. 2).

Discussion

Two major causes of indeterminism of CTPA and misdiagnosis of PE are motion artifacts and poor contrast enhancement [11]. Motion artifacts can be removed by inducing hyperventilation and breath-holding during CT scan time in dogs. Therefore, the most important factor in dogs is contrast enhancement to provide better anatomic detail and characterization of the pathology. It has been generally agreed that increased volume, concentration and injection rate of contrast medium could lead to improved enhancement of vascular structures [6]. A

Table 3. Delay time and Peak time of canine pulmonary arteries (mean ± SD; sec) (n = 24)

	Delay time	Peak time		Delay time	Peak time
MPA	3.25 ± 0.80	6.50 ± 1.31	ACa	4.31 ± 0.92	8.13 ± 1.22
R-MPA	3.25 ± 0.80	6.50 ± 1.31	L-Cda	4.31 ± 0.92	8.13 ± 1.22
L-MPA	3.25 ± 0.80	6.50 ± 1.31	AO	6.81 ± 1.28	11.69 ± 0.96
R-Cda	4.31 ± 0.92	8.00 ± 1.25	CVC	14.38 ± 2.28	18.56 ± 2.65

Table 4. Comparison between groups: Enhanced HU values (mean ± SD) (n = 8 in every group)

	Group 1	Group 2	Group 3	Group 4
MPA	397.00 ± 24.48	537.75 ± 40.72	672.13 ± 101.26	656.00 ± 72.29
R-MPA	390.38 ± 26.23	555.38 ± 68.79	662.63 ± 86.69	685.75 ± 131.23
L-MPA	382.50 ± 25.87	509.13 ± 59.38	647.38 ± 93.39	671.00 ± 137.43
R-Cda	234.63 ± 13.65	311.25 ± 49.31	338.13 ± 50.59	328.63 ± 38.19
L-Cda	237.38 ± 18.33	332.25 ± 13.82	334.75 ± 48.19	320.38 ± 35.43
ACa	248.63 ± 16.91	325.88 ± 7.85	331.63 ± 46.17	314.25 ± 35.85
AO-Cr	332.00 ± 39.59	559.13 ± 48.31	638.00 ± 74.74	618.00 ± 78.68
AO-Md	320.00 ± 38.94	491.88 ± 62.28	614.00 ± 78.43	596.75 ± 75.32
AO-Cd	293.50 ± 45.62	434.75 ± 42.76	604.63 ± 84.36	580.38 ± 87.36
CVC-H	232.63 ± 31.34	286.25 ± 18.40	312.50 ± 38.47	289.13 ± 16.56
CVC-L	209.00 ± 30.43	254.63 ± 30.19	303.50 ± 39.51	283.25 ± 32.38

AO-Cr, aorta in the level of MPA; AO-Md, aorta in the level of R-MPA or L-MPA; AO-Cd, aorta in the level of caudal lobar pulmonary artery.

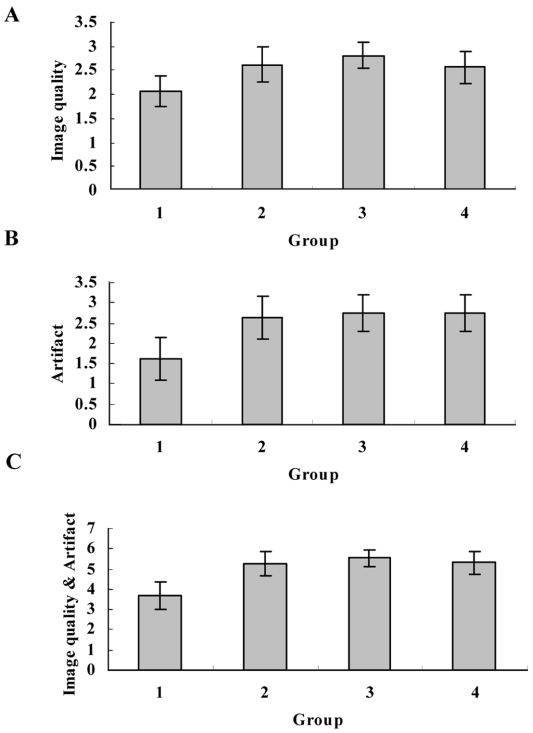

Fig. 1. Comparison with experimental groups for the image quality and artifact factors; (A) image quality, (B) artifact, (C) both image quality and artifacts. Group 1 is lower than other groups in image quality, artifact, and both image quality and artifact ($p < 0.05$).

large amount of contrast medium can provide better organ enhancement, however, the cost is greater and there is possible renal toxicity. Fast injection offers improved arterial enhancement, however, there is question how to ensure a constant degree of pulmonary arterial opacification during the entire spiral sequence. Especially, segmental pulmonary arteries are smaller than other abdominal artery, and PE can be misdiagnosed because of smaller emboli and the effect of artifact. Therefore, since aberrant pulmonary arteries can be relatively small, they need to be sufficiently enhanced so that they are not obscured during 3D threshold-based reconstruction. In this study, 3 parameters were evaluated in normal beagle dogs; contrast injection flow rate, contrast volume, and contrast administration method.

Contrast material injection rates from 2.5 ml/sec to 5.0 ml/sec have been proposed [9, 20, 25]. There were phantom studies that a luminal attenuation of 150 HU gave optimal results for measuring of carotid stenosis and this level of enhancement was easily achieved with

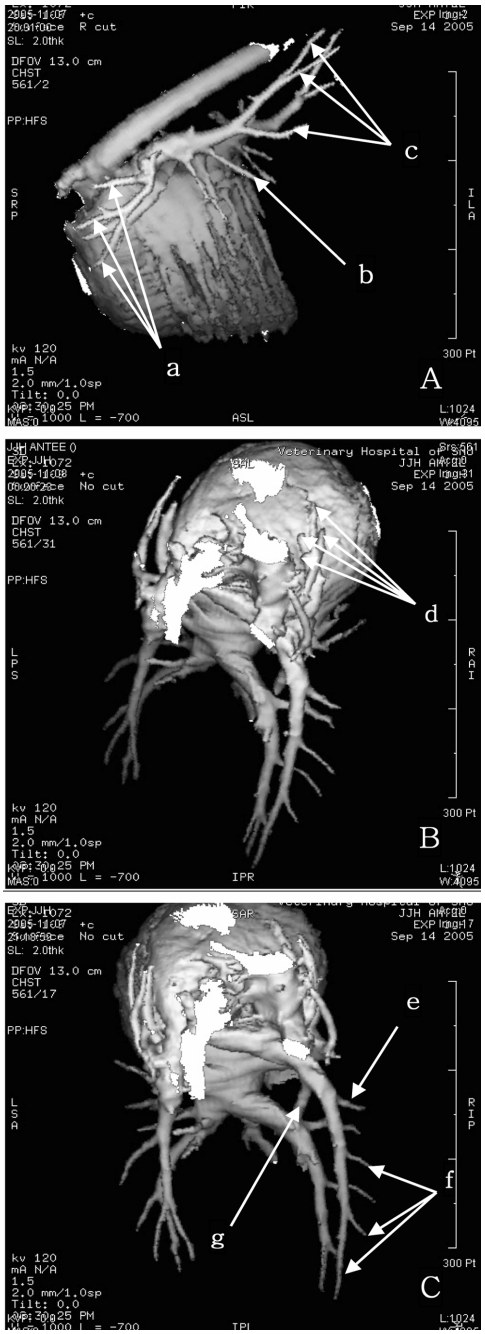

Fig. 2. Major branches of normal canine pulmonary arteries in 3D reconstruction CT images: A; a, three major branches of the cranial part of the left cranial lobe; b, one major branch of the caudal part of the left cranial lobe; c, three major branches of the left caudal lobe. B; d, four major branches of the right cranial lobe. C; e, one major branch of the right middle lobe; f, three major branches of the right caudal lobe; g, one branch of the accessory lobe.

an injection rate of 3~4 ml/sec [2]. For arterial 3D construction, 5 ml/s contrast injection flow rate was necessary to achieve a greater intravascular concentration and therefore a higher CT attenuation [7]. In addition, in this study, 5 ml/s contrast injection flow rate was better than 2 ml/s contrast injection flow rate in higher contrast enhanced HU value and better image quality without artifacts. And using a power injector was mandatory for obtaining a homogeneous and constant level of arterial enhancement through the entire spiral examination. However, there was small volume of local extravasations of contrast material during injection of 5 ml/s in 3 dogs. At enhanced scan using a power injector, mean psi (pressure of contrast injection in power injector) was 78.78±6.09 in 2 ml/s contrast injection flow rate group, 198.33±19.83 in 5 ml/s groups. Therefore, when selecting high-flow protocols of contrast material, care must be taken identifying the central location of the tip of the catheter in the vein after using maximum sized catheter. If patients with suspected hypertension, contrast injection flow rate may be considered reducing the rate of injection and increasing the start delay time.

Contrast volume is also an important factor for CTPA. The volume of contrast used should be adequate to maintain maximal vascular opacification throughout the spiral acquisition. In this study, group 3 with 4 ml/kg contrast volume was the highest contrast enhancement in most arteries. However, contrast injection flow rate was considered more important factor than contrast volume because there were not statistically significant differences among groups 2, 3, and 4. Therefore, group 2 with 5 ml/s contrast injection flow rate and 3 ml/kg contrast volume was selected in following chapters considering the cost of the contrast material.

To compare 2 different techniques for the administration of the bolus of contrast material, group 3 with monophasic protocol and group 4 with biphasic protocol were compared. No significant differences of the attenuation values between group 3 and 4 were observed at the origin of the great vessels and the pulmonary arteries. The attenuation profile of the monophasic protocol showed slightly higher and longer attenuation values than the biphasic protocol. Biphasic administration of contrast material did not supply significant advantages on the enhancement of the great vessels and the pulmonary arteries on CTPA. Therefore, in this study, monophasic administration was selected.

The objective of the spiral protocol is to start scanning while the target vascular structures are opacified and to ensure a constant degree of pulmonary arterial opacification during the entire spiral sequence. Proper timing, 'time delay', from the start of the injection to the start of scanning is essential to ensure imaging at the time of peak intravascular enhancement. Individual test bolus cine scan would permit better results than fixed delay times because of wide variance about optimal delay times in patients [4]. In this study, this delay time was determined by cine CT data and a time-attenuation curve was generated from the adequate vessels in each dogs. As MPA region, the mean delay time was 3.25±0.80 sec, as peripheral segmental pulmonary arteries, the mean delay time was 4.31±0.92 sec when using 5 ml/s contrast injection flow rate.

The orientation of the arteries of interest has an important impact on pulmonary circulation and especially detection of PE on CTPA. In this study, images had reconstruction at 0.5 mm intervals, reformatted images, and 3D images for highest resolution imaging of smaller isolated pulmonary arteries. Small and minor segmental arteries were not found in 3D images. MPA divided into L-MPA and R-MPA. The L-MPA divided into 3 branches. Smaller branches entered the cranial part of the left cranial lobe, divided 3 small segments. The larger branch subdivided and entered the caudal part of the left cranial lobe as one segment. The remainder trunk went to the left caudal lobe and divided 3 segments. The R-MPA left the MPA and coursed to the right. The first branch was the right cranial lobar artery, subdivided four segments. The vessel then divided into the right middle lobar with 2 segmental arteries, accessory lobar with 2 segmental arteries, and right caudal lobar arteries with 3 segmental arteries. There were slight variations of the number and the orientation of major segmental arteries. R-MPA was ventral to the trachea and L-MPA and fell gently and slightly ventrally from MPA than that of L-MPA. Although there was no significant difference, peak time of R-MPA was slight faster than L-MPA. Major branches of cranial lung lobes should bend and turn from main caudal branches. So, this might be explained in this study that why most PE was easily deposited in the right caudal lobar arteries might be explained in this study.

Conclusion

Careful attention to technical details in CTPA including

data acquisition, image processing, and image display was essential in order to consistently produce optimal vascular studies and avoid potential pitfalls. In this study, the optimal contrast delivery method technique, in canine CTPA were 5 ml/s contrast injection flow rate, 3 ml/kg contrast volume, and monophasic administration. Normal basement HU values (mean±SD) for MPA, R-MPA, L-MPA, R-Cra, L-Cra, R-Cda, L-Cda, ACa, and lung parenchyma were 28.33±6.65, 38.83±7.27, 31.72±6.50, 30.60±10.45, 29.05±6.72, 30.44±6.59, 29.61±8.07, 32.83±8.58, and −735.44±119.56, respectively. Enhanced basement HU values for MPA, R-MPA, L-MPA, R-Cda, L-Cda, and ACa were 537.75±40.72, 555.38±68.79, 509.13±59.38, 311.25±49.31, 332.25±13.82, and 325.88±7.85, respectively. The delay time was 3.25±0.80 sec in MPA region and 4.31±0.92 sec in peripheral segmental pulmonary arteries when using 5 ml/s contrast injection flow rate. Pulmonary arteries of each lung lobes were confirmed anatomical locations and orientations through reformatted images and 3D reconstruction after 0.5 mm retro-reconstruction.

References

1. **Baines EA, Watson PJ, Stidworthy MF, Herrtage ME.** Gross pulmonary thrombosis in a greyhound. J Small Anim Pract 2001, **42**, 448-452.
2. **Claves JL, Wise SW, Hopper KD, Tully D, Ten Have TR, Weaver J.** Evaluation of contrast densities in the diagnosis of carotid stenosis by CT angiography. AJR Am J Roentgenol 1997, **169**, 569-573.
3. **Dvorak LD, Preziosi DE, Hitchcock LS.** What is your diagnosis? Acute pulmonary thromboembolism secondary to spontaneous death of adult heartworms. J Am Vet Med Assoc 2000, **217**, 180-181.
4. **Frank P, Mahaffey M, Egger C, Cornell KK.** Helical computed tomographic portography in ten normal dogs and ten dogs with a portosystemic shunt. Vet Radiol Ultrasound 2003, **44**, 392-400.
5. **Godwin JD, Webb WR, Gamsu G, Ovenfors CO.** Computed tomography of pulmonary embolism. AJR Am J Roentgenol 1980, **135**, 691-695.
6. **Han JK, Choi BI, Kim AY, Kim SJ.** Contrast media in abdominal computed tomography: optimization of delivery methods. Korean J Radiol 2001, **2**, 28-36.
7. **Henseler KP, Pozniak MA, Lee FT Jr, Winter TC 3rd.** Three-dimensional CT angiography of spontaneous portosystemic shunts. Radiographics 2001, **21**, 691-704.
8. **Hidaka Y, Hagio M, Murakami T, Okano S, Natsuhori K, Narita N.** Three dogs under 2 years of age with heartworm caval syndrome. J Vet Med Sci 2003, **65**, 1147-1149
9. **Hopper KD, Mosher TJ, Kasales CJ, TenHave TR, Tully DA, Weaver JS.** Thoracic spiral CT: delivery of contrast material pushed with injectable saline solution in a power injector. Radiology 1997, **205**, 269-271.
10. **Johnson LR, Lappin MR, Baker DC.** Pulmonary thromboembolism in 29 dogs: 1985-1995. J Vet Intern Med 1999, **13**, 338-345.
11. **Jones SE, Wittram C.** The indeterminate CT pulmonary angiogram: imaging characteristics and patient clinical outcome. Radiology 2005, **237**, 329-337
12. **Kereiakes DJ, Herfkens RJ, Brundage BH, Gamsu G, Lipton MJ.** Computerized tomography in chronic thromboembolic pulmonary hypertension. Am Heart J 1983, **106**, 1432-1436.
13. **LaRue MJ, Murtaugh RJ.** Pulmonary thromboembolism in dogs: 47 cases (1986-1987). J Am Vet Med Assoc 1990, **197**, 1368-1372.
14. **Liska WD, Poteet BA.** Pulmonary embolism associated with canine total hip replacement. Vet Surg 2003, **32**, 178-186.
15. **McGuire NC, Vitsky A, Daly CM, Behr MJ.** Pulmonary thromboembolism associated with Blastomyces dermatitidis in a dog. J Am Anim Hosp Assoc 2002, **38**, 425-430.
16. **Pape HC.** Pulmonary and systemic fat embolization after medullary canal pressurization: a hemodynamic and histologic investigation in the dog. J Trauma 1999, **47**, 190.
17. **Rawlings CA.** Pulmonary vascular response of dogs with heartworm disease. Can J Comp Med 1978, **42**, 452-459.
18. **Remy-Jardin M, Remy J, Wattinne L, Giraud F.** Central pulmonary thromboembolism: diagnosis with spiral volumetric CT with the single-breath-hold technique comparison with pulmonary angiography. Radiology 1992, **185**, 381-387.
19. **Ritt MG, Rogers KS, Thomas JS**. Nephrotic syndrome resulting in thromboembolic disease and disseminated intravascular coagulation in a dog. J Am Anim Hosp Assoc 1997, **33**, 385-391.
20. **Rubin GD, Lane MJ, Bloch DA, Leung AN, Stark P.** Optimization of thoracic spiral CT: effects of

iodinated contrast medium concentration. Radiology 1996, **201**, 785-791.

21. **Schwickert HC, Schweden F, Schild HH, Piepenburg R, Duber C, Kauczor HU, Renner C, Iversen S, Thelen M.** Pulmonary arteries and lung parenchyma in chronic pulmonary embolism: preoperative and postoperative CT findings. Radiology 1994, **191**, 351-357.
22. **Teigen CL, Maus TP, Sheedy PF 2nd, Johnson CM, Stanson AW, Welch TJ.** Pulmonary embolism: diagnosis with electron-beam CT. Radiology 1993, **188**, 839-845.
23. **Teigen CL, Maus TP, Sheedy PF 2nd, Stanson AW, Johnson CM, Breen JF, McKusick MA**. Pulmonary embolism: diagnosis with contrast-enhanced electron-beam CT and comparison with pulmonary angiography. Radiology 1995, **194**, 313-319.
24. **Terrell SP, Sundeep Chandra AM, Pablo LS, Lewis DD**. Fatal intraoperative pulmonary fat embolism during cemented total hip arthroplasty in a dog. J Am Anim Hosp Assoc 2004, **40**, 345-348.
25. **van Hoe L, Marchal G, Baert AL, Gryspeerdt S, Mertens L.** Determination of scan delay time in spiral CT-angiography: utility of a test bolus injection. J Comput Assist Tomogr 1995, **19**, 216-220.
26. **Venco L, Calzolari D, Morini S.** Pulmonary thromboembolism in a dog with renal amyloidosis. Vet Radiol Ultrasound 1998, **39**, 564-565.